PHYSICAL REVIEW B **76**, 060502(R) (2007)

Fermi arcs in cuprate superconductors: Tracking the pseudogap below T_c and above T^*

J. G. Storey,[1] J. L. Tallon,[1,2] G. V. M. Williams,[2] and J. W. Loram[3]
[1]*School of Chemical and Physical Sciences, Victoria University, P.O. Box 600, Wellington, New Zealand*
[2]*MacDiarmid Institute, Industrial Research Ltd., P.O. Box 31310, Lower Hutt, New Zealand*
[3]*Cavendish Laboratory, Cambridge University, Cambridge CB3 0HE, United Kingdom*
(Received 3 May 2007; published 2 August 2007)

Using an energy-momentum dispersion for $Bi_2Sr_2CaCu_2O_8$ obtained from angle-resolved photoelectron spectroscopy, we show that the shrinking Fermi arc model of the pseudogap is inconsistent with the Raman scattering below T_c and specific heat near T^*. By simulating the quasiparticle energy dispersion curves, we show that Fermi arcs are an artifact of a T-dependent scattering rate.

DOI: 10.1103/PhysRevB.76.060502 PACS number(s): 74.25.Gz, 74.25.Jb, 74.62.Dh, 74.72.−h

The normal-state properties of underdoped high-T_c cuprates are dominated by a gap in the density of states known as the pseudogap (PG).[1,2] Its origin is unknown. Unlike a superconducting gap which *closes* at T_c, angle-resolved photoemission spectroscopy (ARPES) and tunneling in underdoped cuprates have long suggested that the PG *fills* as $(1-T/T^*)$ and disappears abruptly at T^*.[3,4] If so, then the lost low-energy spectral weight would be restored at T^* with important thermodynamic consequences, as we shall see. The gap energy E_g and T^* decrease with increasing doping, falling to zero at a critical doping $p=p_{crit}\approx 0.19$ holes per Cu.[2] Generally T^* is much greater than T_c but when p exceeds ≈ 0.16 then T^* falls below T_c.[5]

Recent ARPES studies[6,7] suggest that for $T<T^*$ the PG covers only part of the Fermi surface (FS) near the $(\pi,0)$ zone boundary. This leaves ungapped arcs on the FS ("Fermi arcs") which grow with increasing T. The arcs extend to an angle θ_0 given by $\theta_0=(\pi/4)(1-T/T^*)$, where θ_0 is measured from $(\pi,0)$. The gap is thus nodal at $T=0$ and, with increasing T, retreats toward $(\pi,0)$, where it closes abruptly at T^*. To describe the PG state, Varma has introduced a time and rotational symmetry-breaking transition which reproduces the phenomenology of the Fermi arcs[8] and generally accounts for the specific heat.[9] But, assuming that the PG continues to exist as the underlying normal state below T_c, the T-dependent restoration of the pristine FS would have important testable consequences, as follows.

(i) If the PG retreats abruptly to $(\pi,0)$ at T^*, the specific heat coefficient γ will exhibit an anomaly. The area under the anomaly is exactly equal to the restored entropy. We calculate this below for several Fermi arc scenarios and show that this is not observed in the experimental data.

(ii) If the Fermi arcs grow as T rises then the spectral weight taken up by the PG falls. So the superfluid density would first increase, then fall as T approaches T_c, contrary to the observed monotonic decrease.[10]

(iii) If the PG closes at T^* then in the doping range $0.16<p<0.19$, where $T^*\leqslant T_c$, the PG should be open at $T=0$ but closed when $T=T_c$. Again, this is not observed, as we show in Fig. 1. Here $T_c(p)$ and $T^*(p)=E_g/2k_B$ are plotted for $Bi_2Sr_2CaCu_2O_{8+\delta}$ (Bi-2212). Figure 1(a) shows two properties at T_c: the jump in $\Delta\gamma$ and the electronic entropy $S(T_c)$. Figure 1(b) shows two ground-state $T=0$ properties: the superfluid density λ_0^{-2} and x_{crit}, the critical density of Zn required to suppress T_c. The data are from Tallon *et al.*[11] The two vertical dashed lines show the region where $T^*\leqslant T_c$. In Fig. 2(b) both ground-state properties abruptly decrease when the PG opens at p_{crit}. Now if the PG were to fully close at T^* then the two $T=T_c$ properties displayed in Fig. 1(a) should not begin to fall until $T^*=T_c$, i.e., at the vertical line at $p\approx 0.16$. They do not. In fact, like the ground-state properties, they fall abruptly at $p_{crit}=0.19$. This suggests a relatively T-independent loss of spectral weight due to the PG below T_c, impacting roughly equally on ground-state and $T=T_c$ properties. The Fermi arcs, if they exist, cannot continue to collapse around the nodes.

Here we explore these points further. We first consider the low-T behavior of the Fermi arcs by calculating the Raman response. Below T_c the superconducting (SC) gap opens up on the Fermi arcs, thereby obscuring the details of how the PG further evolves with T, and in particular whether the PG itself becomes nodal at $T=0$. Raman scattering allows the PG and SC gaps to be separately probed via the antinodal (B_{1g}) and nodal (B_{2g}) Raman responses.[12–14] We calculate these for Bi-2212 using an ARPES-derived energy-momentum dispersion. By comparing with Raman data we

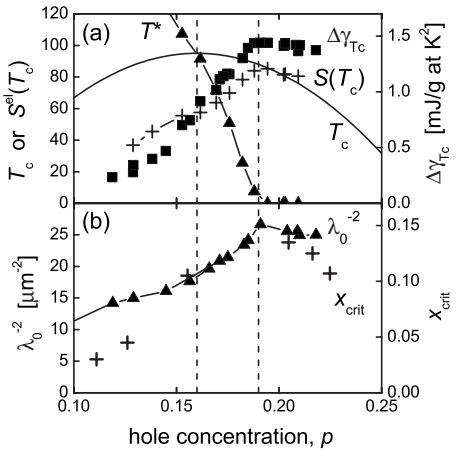

FIG. 1. Thermodynamic data for Bi-2212. (a) Two properties at T_c: the jump in specific heat coefficient $\Delta\gamma$ and the electronic entropy $S(T_c)$ in mJ/g at. K; and (b) two properties at $T=0$: the superfluid density λ_0^{-2} and x_{crit}, the critical Zn concentration giving $T_c=0$. Vertical dashed lines indicate where $T^*=T_c$ and $p_{crit}=0.19$, where the PG closes.

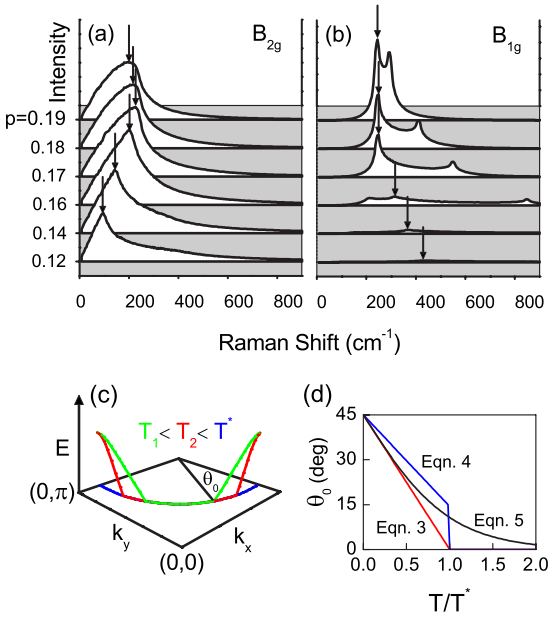

FIG. 2. (Color online) Calculated Raman response at $T=0$ for a Fermi arc length fixed below T_c: (a) nodal B_{2g} and (b) antinodal B_{1g} symmetry. Arrows show positions of SC and PG gap features. (c) PG and Fermi arc given by Eq. (2) at temperatures T_1 and T_2. (d) $\theta_0(T)$ from Eqs. (3)–(5).

are able to confirm that the PG does not evolve significantly below T_c.

We then turn to the second issue as to how the PG evolves near T^*. Does it really close at T^* as widely believed? We use the same dispersion to calculate the specific heat and show that the Fermi arc model leads to a large anomaly in $\gamma(T)$ at T^* that is not observed. We go on to suggest that these issues may be resolved by incorporating quasiparticle (QP) lifetime broadening.

We employ the six-parameter tight-binding Bi-2212 dispersion $\epsilon(\mathbf{k})$ reported by Norman *et al.*[15] and assume a rigid single-band approximation. Inclusion of band splitting[16] will not significantly affect the following results. We take the Fermi level to be 34 meV above the $(\pi,0)$ van Hove singularity (vHS) near optimal doping[15] and 96 meV above the vHS in an underdoped sample with $p=0.11$.[17] We interpolate between them for intermediate doping levels. The imaginary part of the unscreened nonresonant Raman response at $T=0$ is given by[18]

$$\chi_0''(q=0,\omega)=\int \frac{d^2k}{(2\pi)^2}\delta(\omega-2E(\mathbf{k}))\frac{|\Delta(\mathbf{k})|^2}{E(\mathbf{k})^2}|\gamma(\mathbf{k})|^2, \quad (1)$$

where the integral is over occupied states below E_F, $\Delta(\mathbf{k})=\frac{1}{2}\Delta_0(\cos k_x-\cos k_y)$ is the d-wave SC gap function, and $E(\mathbf{k})=\sqrt{\epsilon(\mathbf{k})^2+|\Delta(\mathbf{k})|^2}$. In the B_{1g} scattering symmetry $\gamma(\mathbf{k})^{B_{1g}}=\gamma B_{1g}(\cos k_x-\cos k_y)$, giving a dominant response from the antinodal sections of the FS. For B_{2g}, $\gamma(\mathbf{k})^{B_{2g}}=\gamma B_{2g}\sin k_x \sin k_y$ and the response is mainly nodal. The magnitude of the SC gap, Δ_0, is taken from the weak-coupling result $2\Delta_0=4.28k_BT_c$ and T_c is given by the empirical relation[19] $T_c/T_{c,max}=1-82.6(p-0.16)^2$. We adopt a PG of the form

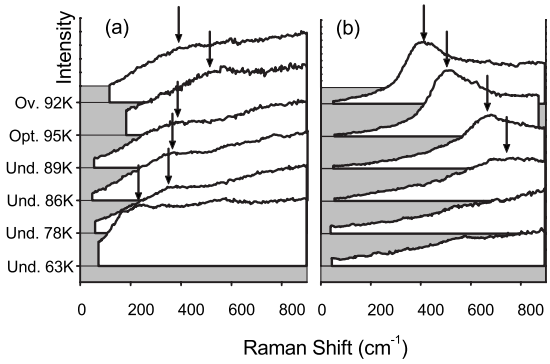

FIG. 3. Experimental Raman data for $HgBa_2CuO_{4+\delta}$ from Le Tacon *et al.* (Ref. 12) (a) B_{2g} and (b) B_{1g} response for $T \ll T_c$.

$$E_g=\begin{cases} E_{g,max}\cos\left(\dfrac{2\pi\theta}{4\theta_0}\right), & (\theta<\theta_0), \\ E_{g,max}\cos\left(\dfrac{2\pi(\theta-\pi/2)}{4\theta_0}\right), & \left(\theta>\dfrac{\pi}{2}-\theta_0\right), \\ 0 & \text{otherwise}, \end{cases} \quad (2)$$

where $0\leqslant\theta\leqslant\pi/2$. We initially assume

$$\theta_0=\frac{\pi}{4}\left(1-\frac{T}{T^*}\right) \quad (T<T^*) \quad (3)$$

and $T^*=E_{g,max}/k_B$. This form of the PG is illustrated in Figs. 2(c) and 2(d). Equation (3) models the linear T dependence of the Fermi arc length inferred from ARPES.[7] At $T=0$, $\theta_0=\pi/4$ and the PG is fully nodal. As T rises, θ_0 decreases, resulting in a filling in of the PG and the growth of the Fermi arcs. The PG is a non-states-conserving gap,[20] i.e., unlike the SC gap, there is no pileup of states outside the gap. This is implemented by removing states with $\epsilon(\mathbf{k})<E_g$ from the integration in Eq. (1). The doping dependence of E_g is obtained from the reported leading-edge ARPES gap at 100 K.[2]

Figure 2(a) and 2(b) show the nodal (B_{2g}) and antinodal (B_{1g}) Raman response for six dopings spanning the range 0.12 to 0.19. We consider two scenarios.

(i) First, we have assumed that the length of the Fermi arc becomes fixed at the onset of superconductivity, implemented by setting $T=T_c$ in Eq. (3). Figure 2(a) shows the nodal (B_{2g}) response. Leaving aside the anomalous electronic Raman continuum above the pair-breaking gap, the calculations closely resemble the recent results of Le Tacon *et al.*[12] which are reproduced in Fig. 3. The PG peak maximum in the B_{1g} response shifts monotonically to higher energies with decreasing doping. Simultaneously, the intensity of this peak rapidly decreases with underdoping. In contrast, the SC peak maximum in the B_{2g} response is found to shift to lower energies in the underdoped regime. The magnitude of

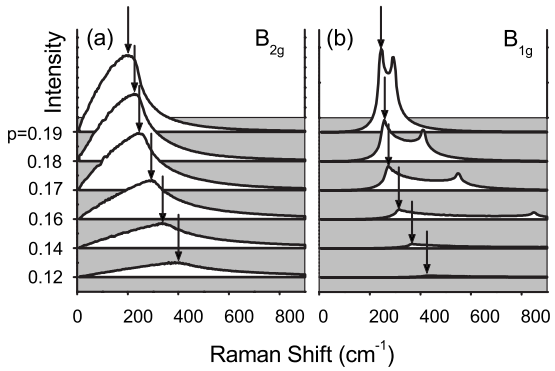

FIG. 4. Calculated Raman response at $T=0$ with a fully nodal PG for (a) nodal B_{2g} and (b) antinodal B_{1g} symmetry. The intensity scale is the same for all plots.

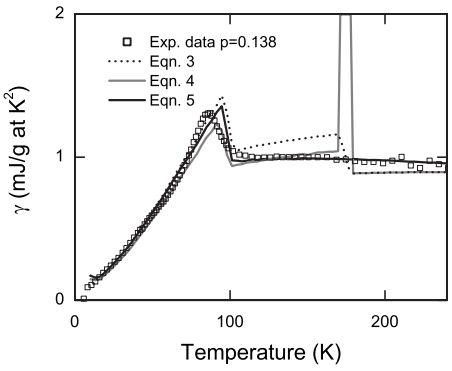

FIG. 5. Specific heat coefficient calculated for θ_0 given by Eqs. (3)–(5) and compared with the experimental data for Bi-2212 (Ref. 20), where every 10th data point is shown.

the B_{2g} peak persists relatively undiminished down to the lowest doping levels. Also reproduced is the increased linear slope of the response at very low doping.

(ii) Second, we show in Fig. 4 the Raman response in the alternative case where we have assumed that the Fermi arcs continue to collapse below T_c. This is done by setting $T=0$ in Eq. (3), resulting in a fully nodal PG. In this case the B_{2g} peak shifts monotonically to higher energies with decreasing doping and the intensity decreases rapidly. This behavior is not observed experimentally. We cannot say that the Fermi arc freezes exactly at T_c but our analysis indicates that it remains finite at $T=0$ and evolves only weakly below T_c.

We turn now to the question as to how the PG evolves above T_c as $T \rightarrow T^*$. It is widely assumed that the PG closes at T^*, as indeed Eq. (3) suggests, thus exposing a pristine FS. In fact, Kanigel *et al.*[7] suggest that a discrete jump in θ_0 occurs at T^* so that the PG retreats to the flat sections of the FS near $(\pi,0)$, from whence it abruptly disappears at $T=T^*$. This model is given by

$$\theta_0 = \begin{cases} \frac{\pi}{4}\left(1 - 0.68\frac{T}{T^*}\right) & (T < T^*) \\ 0 & (T \geqslant T^*) \end{cases} \tag{4}$$

and is illustrated in Fig. 2(d). The closure of the PG, whether according to Eq. (3) or Eq. (4), will restore the entropy to the bare-band value. This, quite generally, will result in a γ anomaly, the area of which equals the restored entropy. The lower T^*, the greater the anomaly. We evaluate this here.

Using the method described previously,[10] together with the above tight-binding dispersion, we have computed $\gamma(T)$ for three cases with $p \approx 0.138$. In Fig. 5 we compare these with experimental data for Bi-2212. The three cases are shown in Fig. 2(d). They are (i) the linear behavior described by Eq. (3); (ii) the sudden jump in θ_0 inferred by Kanigel *et al.* and described by Eq. (4); and (iii) the smooth evolution of the gap given by[10]

$$\theta_0 = \frac{\pi}{4}\left[1 - \tanh\left(\frac{T}{T^*}\right)\right]. \tag{5}$$

As can be seen, cases (i) and (ii) lead to substantial anomalies in γ which are clearly not found experimentally. The experimental data, shown by the data points, are from a previous study[20] on the specific heat of Bi-2212 with the closest corresponding doping state. The smooth evolution of the PG given by Eq. (5) satisfactorily describes the data and generally discounts the possibility that the PG closes abruptly at T^*.

We have so far shown that (i) below T_c the Fermi arcs do not continue to shrink notably; and (ii) above T_c the Fermi arcs cannot spread out to abruptly form a connected pristine FS at T^*. (iii) Both results are confirmed by the data in Fig. 1 in the interesting case where T^* lies below T_c. These problems seriously prejudice the current picture of Fermi arcs but could be resolved as follows by invoking a T-dependent scattering rate.

First, one is led to this view by the observations of Norman *et al.*[21] They modeled the QP peak using a QP self-energy with a scattering rate or inverse lifetime Γ_0 which, in underdoped samples, grows with T and equals the gap magnitude precisely at T^* [see Fig. 2(b) of Ref. 21]. This would lead to a smearing out of the gap at E_F resulting in a single peak in the dispersion at E_F that looks like a recovered pristine FS. But of course the gap is still there, and interestingly is reported to be T independent, just as we concluded above.

In Fig. 6 we have simulated the symmetrized QP energy distribution curves (EDCs) as the sum of two Lorentzians. We use a fixed broadening of $0.45E_g(0)$, corresponding to a particular temperature below T^*. The k-dependent gap value, $E_g(\theta)$, is assumed to be d-wave-like with $E_g(\theta) = E_g(0)\cos(2\theta)$. Fifteen angles ranging from $\theta=0$ (the antinode) to $\theta=45°$ (the node) are shown and the data qualitatively reproduce the reported experimental data.[7,21] These EDCs reveal a crossover from double to single peaks, with the flat bold curve lying at the boundary. Within the Fermi arc model this would be interpreted as a closure of the PG at $\theta \approx 30°$ with a pristine Fermi arc extending from $\theta=30°$ to 45°. But, as shown in inset (a) of Fig. 6, the *true* gap does not close until the node at $\theta=45°$. The *apparent* gap, found by reading off the peak positions, is also plotted in inset (a) and this falls to zero at $\theta=30°$. We also show the apparent gap for a larger broadening $[=0.6E_g(0)]$ which would correspond to a higher temperature, closer to T^*. Here the apparent gap closes at 23°.

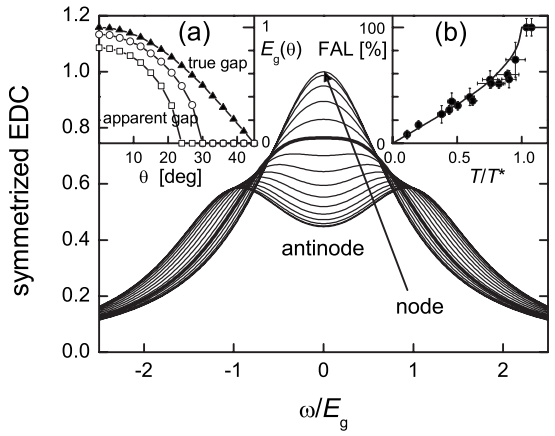

FIG. 6. Simulated symmetrized ARPES quasiparticle EDCs ranging from the antinode to the node (θ=0 to 45°). The broadening is fixed at $0.45E_g(0)$. The crossover from double to single peaks (bold curve) presents an apparent, though false, closing of the PG and recovery of Fermi arcs. Inset (a) shows the true normalized gap and apparent gap for two broadenings [=$0.45E_g$ and $0.6E_g(0)$]. (b) Curve, apparent Fermi arc length (FAL) assuming broadening $\propto T/T^*$; data from Ref. 7.

Inset (b) in Fig. 6 shows the apparent (though fictitious) Fermi arc length obtained from these simulated EDCs when the broadening $\Gamma=\Gamma^*(T/T^*)$, where Γ^* is the critical value that "closes" the gap at the antinode. The arc length exhibits a rapid change at T^* just like the data of Kanigel *et al.*,[7] which are also plotted. This rapid change arises from the flat part of the *d*-wave gap when $\theta \to 0$ and does not signal an abrupt recovery of the FS.

Thus QP lifetime broadening with a *d*-wave gap accounts for all apparent Fermi arc features, including the abrupt jump in arc length reflected in Eq. (4). We expect therefore that the T variation of the PG is not in Fermi arcs but in the scattering rate. Both the PG and the SC gap parameters should be replaced by complex terms of the form $E_g(\theta) \to E_g(\theta)/[1 - i\Gamma_1/\epsilon(k)]$ and $\Delta(\theta) \to \Delta(\theta)/[1 - i\Gamma_0/\epsilon(k)]$. This naturally leads to a U-shaped gap,[22] and instead of frozen Fermi arcs below T_c the Raman data would then insist on a frozen scattering rate.

In summary, we have used an $\epsilon(\mathbf{k})$ dispersion and a model for the normal-state PG, both based on ARPES results, to show that the shrinking Fermi arc picture is inconsistent with Raman data below T_c and thermodynamic data near T^*. Only by freezing the length of the Fermi arcs at or near T_c do we find that the calculations mimic the experimental data. This implies that the PG does not evolve greatly below T_c. We have further shown that closure of the PG at T^* and the associated recovery of a pristine FS would lead to a large specific heat anomaly that is not observed. We thus question the concept of Fermi arcs and suggest that they are probably an artifact of a T-dependent lifetime scattering rate.

We thank the Marsden Fund for financial support.

[1] M. R. Norman, D. Pines, and C. Kallin, Adv. Phys. **54**, 715 (2005).
[2] J. L. Tallon and J. W. Loram, Physica C **349**, 53 (2001).
[3] J. M. Harris, Z. X. Shen, P. J. White, D. S. Marshall, M. C. Schabel, J. N. Eckstein, and I. Bozovic, Phys. Rev. B **54**, R15665 (1996).
[4] C. Renner, B. Revaz, J. Y. Genoud, K. Kadowaki, and O. Fischer, Phys. Rev. Lett. **80**, 149 (1998).
[5] S. H. Naqib, J. R. Cooper, J. L. Tallon, R. S. Islam, and R. A. Chakalov, Phys. Rev. B **71**, 054502 (2005).
[6] M. R. Norman, H. Ding, M. Randeria, J. C. Campuzano, T. Yokoya, T. Takeuchi, T. Takahashi, T. Mochiku, K. Kadowaki, P. Guptasarma, and D. G. Hinks, Nature (London) **392**, 157 (1998).
[7] A. Kanigel, M. R. Norman, M. Randeria, U. Chatterjee, S. Souma, A. Kaminski, H. M. Fretwell, S. Rosenkranz, M. Shi, T. Sato, T. Takahashi, Z. Z. Li, H. Raffy, K. Kadowaki, D. Hinks, L. Ozyuzer, and J. C. Campuzano, Nat. Phys. **2**, 447 (2006).
[8] C. M. Varma and L. Zhu, Phys. Rev. Lett. **98**, 177004 (2007).
[9] C. M. Varma, Phys. Rev. B **73**, 155113 (2006).
[10] J. G. Storey, J. L. Tallon, and G. V. M. Williams, arXiv:0704.2432 (2007).
[11] J. L. Tallon, J. W. Loram, J. R. Cooper, C. Panagopoulos, and C. Bernhard, Phys. Rev. B **68**, 180501(R) (2003).
[12] M. Le Tacon, A. Sacuto, A. Georges, G. Kotliar, Y. Gallais, D. Colson, and A. Forget, Nat. Phys. **2**, 537 (2006).
[13] M. Opel, R. Nemetschek, C. Hoffmann, R. Philipp, P. F. Müller, R. Hackl, I. Tüttõ, A. Erb, B. Revaz, E. Walker, H. Berger, and L. Forró, Phys. Rev. B **61**, 9752 (2000).
[14] X. K. Chen, J. G. Naeini, K. C. Hewitt, J. C. Irwin, R. Liang, and W. N. Hardy, Phys. Rev. B **56**, R513 (1997).
[15] M. R. Norman, M. Randeria, H. Ding, and J. C. Campuzano, Phys. Rev. B **52**, 615 (1995).
[16] A. Kaminski, S. Rosenkranz, H. M. Fretwell, M. R. Norman, M. Randeria, J. C. Campuzano, J. M. Park, Z. Z. Li, and H. Raffy, Phys. Rev. B **73**, 174511 (2006).
[17] A. A. Kordyuk, S. V. Borisenko, M. Knupfer, and J. Fink, Phys. Rev. B **67**, 064504 (2003).
[18] F. Wenger and M. Kall, Phys. Rev. B **55**, 97 (1997).
[19] M. R. Presland, J. L. Tallon, R. G. Buckley, R. S. Liu, and N. E. Flower, Physica C **176**, 95 (1991).
[20] J. W. Loram, J. Luo, J. R. Cooper, W. Y. Liang, and J. L. Tallon, J. Phys. Chem. Solids **62**, 59 (2001).
[21] M. R. Norman, M. Randeria, H. Ding, and J. C. Campuzano, Phys. Rev. B **57**, R11093 (1998).
[22] S. V. Borisenko, A. A. Kordyuk, T. K. Kim, S. Legner, K. A. Nenkov, M. Knupfer, M. S. Golden, J. Fink, H. Berger, and R. Follath, Phys. Rev. B **66**, 140509(R) (2002).